Ecological Modelling 254 (2013) 33–42

Contents lists available at SciVerse ScienceDirect

Ecological Modelling

journal homepage: www.elsevier.com/locate/ecolmodel

Internal dynamics of NPZD type ecosystem models

A. Heinle*, T. Slawig

Cluster "The Future Ocean", Institute of Computer Science, Christian-Albrechts University, 24098 Kiel, Germany

ARTICLE INFO

Article history:
Received 20 September 2012
Received in revised form 8 January 2013
Accepted 11 January 2013
Available online 21 February 2013

Keywords:
Marine ecosystem
Model
Dynamics
Equilibria
Quality

ABSTRACT

The marine ecosystem is an essential part of the Earth's carbon cycle. Therefore, to create model-based scenarios of the future of the Earth's climate, it is inevitable to consider the relevant processes of this system within numerical simulations. In the last two decades, a wide range of submodels of varying complexity have been established representing the marine ecosystem. Their specific behaviour and characteristic responses to, e.g., external forcings, however, are only merely understood. In this study, we present a mathematical method to assess the fundamental behaviour of such models. Three marine ecosystem models of NPZD type, varying in their formulation of phytoplankton loss and zooplankton loss, are analyzed. Following the qualitative theory of dynamical systems, model specific behaviours as well as similarities of the individual models are revealed. For each model, three equilibria are detected and their stability properties are analyzed. Parameters that significantly affect the model solutions are pointed out. Parameter constellations and initial values that cause characteristic model behaviours are determined and discussed. The results obtained provide the basic, theoretical knowledge which is essentially needed to use models in an effective and appropriate way.

1. Introduction

The future of the Earth's climate is of main interest in research and policy, at least since it has been realized that industrial processes and other anthropogenic interventions cause non-natural changes. A key factor affecting the climate is the greenhouse gas carbon dioxide (CO_2). Its concentration in atmosphere and ocean has significantly changed during the last decades and its prospective development in the near and remote future is much debated.

In climate science, numerical models are used to generate scenarios simulating the effects of various environmental conditions on the development of the Earth's climate. Among others, the impact of increasing CO_2 concentrations on biosphere and individual ecosystems in atmosphere and oceans is investigated since those significantly affect the Earth's carbon cycle. For example, the marine ecosystem is treated in many numerical models since primary production of marine phytoplankton is a main driver of the CO_2 cycle.

Nowadays numerous models simulating the relevant processes in the marine ecosystems exist. They range from very simple ones, that calculate the concentrations of two or three components, to highly complex models that include, e.g., multiple nutrients and various plankton types (Moore et al., 2002; Gregg et al., 2003; Gibson et al., 2005; Fasham et al., 2006; Hinckley et al., 2009). One of the medium complex models is the NPZD type model. Due to its rather simple framework and simultaneously quite realistic representation of the marine ecosystem this type of model is frequently applied in climate research.

NPZD models simulate the interactions of the four variables nutrients (N), phytoplankton (P), zooplankton (Z) and detritus (D). The mathematical formulation of the internal fluxes varies in kind and complexity. For example, the growth of phytoplankton can be modelled to be limited by nutrients only, to be limited additionally by light or even by more factors (Denman and Peña, 1999; Oschlies and Garçon, 1999; McCreary et al., 2001; Fennel et al., 2001; Kawamyko, 2002; Spitz et al., 2003; Losa et al., 2006; Pahlow et al., 2008). Further terms varying in their formulation and known to be highly relevant for the model outcome are the closing terms of phytoplankton and zooplankton. Often, they are modelled by linear functions like in the model of Denman and Peña (1999). Other authors opine that this is not realistic enough and that more complex formulations are necessary, such as quadratic closing terms or terms of even higher order (Fennel et al., 2001; Edwards, 2001; Losa et al., 2006). A detailed discussion on several closing terms of zooplankton in the use of more simple models is found in Murray and Parslow (1999).

The large variety of ecosystem models and their formulations makes it extremely difficult to find the model best, or at least well, suited to address a specific problem. Data assimilation is a common method used to check whether a model is meaningful for a given task or not. Therein, the coincidence of model results and data,

* Corresponding author. Tel.: +49 431 880 7338; fax: +49 431 880 7618.
E-mail address: ahe@informatik.uni-kiel.de (A. Heinle).
URL: http://www.informatik.uni-kiel.de/co2 (A. Heinle).

0304-3800/$ – see front matter © 2013 Elsevier B.V. All rights reserved.
http://dx.doi.org/10.1016/j.ecolmodel.2013.01.012

mostly observational data, is analyzed using optimization techniques (e.g., Fennel et al., 2001; Schartau and Oschlies, 2003; Fan and Lvasham, 2009; Rückelt et al., 2010). While this approach is reasonable, it does not provide an understanding of the model itself and its internal dynamics. For example, in case unsatisfying optimization results are obtained it is not clear what might have caused them and whether the model is unreliable at all, or whether a small modification would lead to a significant improvement. Further, data assimilation techniques are computationally expensive. Due to the need of several model runs in an optimization process, these costs particularly increase significantly with increasing model complexity. Thus, to keep data assimilation techniques efficiently, especially in case complex models should be evaluated, restrictions on the parameter space and on the initial values might be helpful.

To overcome this gap, we follow a more theoretical approach to analyze the feasibility of a model to be used for a certain objective. Focusing on equilibrium states of the modelled variables, the basic dynamics of a model can be exposed. Limits of the model framework considered as well as information on the respective parameter space can be obtained. In particular, parameter and initial value dependencies can be identified.

In this study we investigate three marine ecosystem models of NPZD type. They are all based on the same mathematical framework following the model formulation of Oschlies and Garçon (1999), but differ in their representation of phytoplankton and zooplankton loss. Analyzing this three model versions, we aim to identify characteristics of each closing term. Limits of the individual formulations, caused by parameter or initial value restrictions, are pointed out. We mainly focus on the impact of varying initial values in this study. A detailed parameter survey is done as well, but its presentation exceeds the scope of this paper.

The paper is structured as follows: In Section 2 a general formulation of the three NPZD models is given and the processes included, together with their corresponding mathematical expressions, are explained. This is followed by a separate elucidation of the individual models. In Section 3 the equilibrium solutions, separately determined for each model, are presented. In Section 4, the stability properties of the individual equilibria are analyzed and discussed. A summary and conclusions of the results complete the study in Section 5.

2. Models

Three marine ecosystem models of NPZD type are analyzed in this study. NPZD type models simulate the concentrations of the following four marine ecosystem components: Dissolved inorganic nitrogen (N), phytoplankton (P), zooplankton (Z) and detritus (D) given in mmol N m^{-3}. All three models are defined by an initial value problem (IVP) that is generally defined by

$$y' = f(y,t) \quad \text{with} \quad y(t_0) = y_0. \tag{1}$$

In our case, the state variables N, P, Z and D are represented by the vector $y = (N, P, Z, D)$. Their initial values are summarized in y_0 and are chosen in accordance to measured data. In our models, Eq. (1) represents a system of coupled, nonlinear ordinary differential equations (ODEs) that describe the internal dynamics of the variables. The difference between the three models presented in the following are in these ODE systems, in particular in the loss terms of zooplankton and phytoplankton. While the first model, model LLM, assumes a linear mortality of both, phytoplankton and zooplankton, the second model, model LQM, contains an additional, quadratic loss term of zooplankton. The third model, model QQM, finally considers linear and quadratic mortalities of both variables. Schemes of the individual model setups are shown in Fig. 1.

2.1. Models LLM and LQM

The dynamics of the first two models, models LLM and LQM, are described by Eq. (2). They just differ in the setting of the parameter Φ_Z^*. In model LLM the quadratic loss of zooplankton is neglected, thus it holds $\Phi_Z^* = 0$. The second model, model LQM, in contrast postulates $\Phi_Z^* > 0$.

$$\begin{aligned}
\frac{\partial N}{\partial t} &= -J(N,I)P + \Phi_Z Z + \gamma_m D,\\
\frac{\partial P}{\partial t} &= (J(N,I) - \Phi_P)P - G(\epsilon, g, P)Z,\\
\frac{\partial Z}{\partial t} &= (\beta G(\epsilon, g, P) - \Phi_Z - \Phi_Z^* Z)Z,\\
\frac{\partial D}{\partial t} &= \Phi_P P + ((1-\beta)G(\epsilon, g, P) + \Phi_Z^* Z)Z - \gamma_m D.
\end{aligned} \tag{2}$$

All parameters appearing in Eq. (2) are defined and explained in Table 1. Except those, two nonlinear functions arise in system (2), $J = J(N, I)$ and $G = G(\epsilon, g, P)$. They are elucidated below. The parameters therein are found in Table 1 as well.

2.1.1. Modelling of phytoplankton growth

The growth of phytoplankton is dependent on the light (I) and the amount of nutrients (N) available. In our models, this is expressed by the function $J = J(N, I)$ occurring in the first two equations of the ODE systems given in Eqs. (2) and 3. Function J is composed of two monotonously increasing functions f_I and f_N that are formulated according to Michaelis–Menten and that describe the present light and nutrient conditions separately. In case capacity limited processes are modelled, as in the present case, Michaelis–Menten formulations are frequently found (López-Fidalgo and Wong, 2002). A maximum growth rate is weighted by one or more saturation terms. In our models, those are the two terms representing the current nutrient and light limitation,

$$f_N(N) = \frac{N}{k_N + N} \quad \text{and} \quad f_I(I) = \frac{I}{k_I + I}.$$

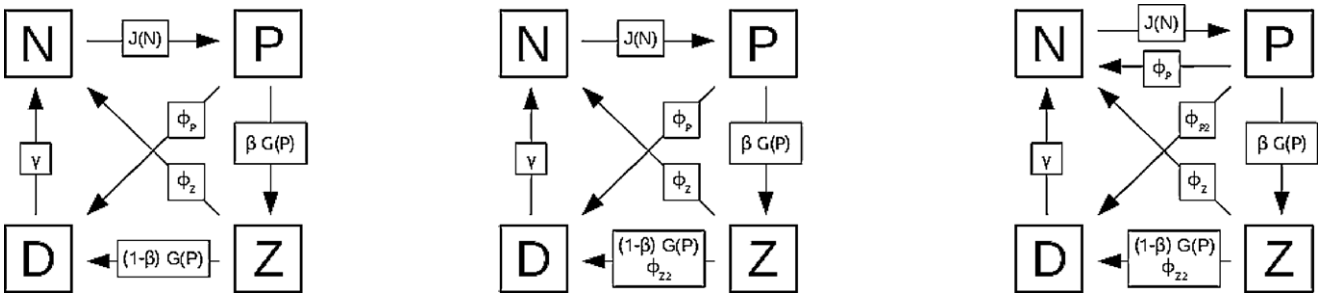

Fig. 1. Schemes of the coupling between the model variables N, P, Z and D for model LLM (left), model LQM (middle) and model QQM (right). Arrows indicate a nitrogen flux from one to another component.

Table 1
Model parameters. Units and definitions are given as well as the parameter set u^* exemplary used for illustrations in this study.

Symbol	Value/range	Unit	u^*	Definition
C_{ref}	1.066	1		Growth coefficient of phytoplankton
c	1	°C		Growth coefficient of phytoplankton
β	[0, 1]	1	0.925	Assimilation efficiency of zooplankton
α	$\mathbb{R}_+$	$m^2\,W^{-1}\,d^{-1}$	0.256	Slope of photosynthesis vs. light intensity
μ_m	$\mathbb{R}_+$	d^{-1}	0.270	Phytoplankton growth rate
Φ_P	$\mathbb{R}_+$	d^{-1}	0.040	Phytoplankton linear mortality
Φ_P^*	$\mathbb{R}_+$	d^{-1}	0.025	Phytoplankton quadratic loss rate
ϵ	$\mathbb{R}_+$	$m^6\,(mmol\,N)^{-2}\,d^{-1}$	1.600	Grazing encounter rate
g	$\mathbb{R}_+$	d^{-1}	1.575	Maximum grazing rate
Φ_Z	$\mathbb{R}_+$	d^{-1}	0.010	Zooplankton linear loss rate
Φ_Z^*	$\mathbb{R}_+$	$m^3\,(mmol\,N)^{-1}\,d^{-1}$	0.340	Zooplankton quadratic mortality
γ_m	$\mathbb{R}_+$	d^{-1}	0.048	Detritus remineralization rate
k_N	$\mathbb{R}_+$	$mmol\,N\,m^{-3}$	0.700	Half saturation constant for NO_3 uptake
k_I	$\mathbb{R}_+$	$W\,m^{-3}$		Half saturation constant for light

The final growth rate $J(N, I)$ is then the product of the maximum growth rate of phytoplankton, μ_m, and the two functions presented above,

$$J(N, I) = \mu_m \cdot f_N(N) \cdot f_I(I).$$

Note, technically, the present light, given by I, is a function itself that includes the parameters C_{ref}, c and α. In our analysis, however, these parameters are constant and therefore, they are not discussed in detail. For more information and alternative formulations of the light limitation (see e.g., Schartau and Oschlies, 2003).

2.1.2. Modelling of zooplankton grazing

As for the growth of phytoplankton there are various formulations depicting the grazing of zooplankton on phytoplankton. In this study, a Holling type III function (see Fasham, 1995) is applied, given by

$$G(\epsilon, g, P) = \frac{g\epsilon P^2}{g + \epsilon P^2}.$$

For an explication of the parameters see Table 1.

2.2. Model QQM

In addition to the quadratic loss of zooplankton in model LQM, model QQM contains a quadratic loss of phytoplankton. This additional loss can be considered as a parameterization of various processes as aggregation of phytoplankton cells and immediate, viral infection with subsequent cell lysis, grazing by herbivores, etc. (see Kriest et al., 2010). To keep the additional parameterization consistent with the real world, in particular with the pathways of nitrogen in the marine ecosystem, a modification of the governing ODE system is necessary. The linear loss of phytoplankton is no more added to the compartment of detritus, but to the section of nutrients. Detritus instead gains mass by the quadratic loss of phytoplankton. The resulting ODE system is given in Eq. (3).

$$\begin{aligned}
\frac{\partial N}{\partial t} &= (-J(N, I) + \Phi_P)P + \Phi_Z Z + \gamma_m D,\\
\frac{\partial P}{\partial t} &= (J(N, I) - \Phi_P - \Phi_P^* P)P - G(\epsilon, g, P)Z,\\
\frac{\partial Z}{\partial t} &= (\beta G(\epsilon, g, P) - \Phi_Z - \Phi_Z^* Z)Z,\\
\frac{\partial D}{\partial t} &= \Phi_P^* P^2 + ((1-\beta)G(\epsilon, g, P) + \Phi_Z^* Z)Z - \gamma_m D.
\end{aligned} \tag{3}$$

Except for the variations mentioned, model QQM is based on the same mathematical assumptions as the first two models, models LLM and LQM. Thus, the mathematical formulation of the non-constant growth and grazing rates explained above and the parameter constraints given in Table 1 are valid for model QQM as well.

3. Equilibrium solutions

To analyze the dynamics of the models presented and to point out individual model characteristics, methods of the qualitative theory of ordinary differential equations are used. The detection of equilibria and the analysis of their stability properties are one of the basic and most important methods to gain insight in the dynamics of an ODE system and thus in our models.

In our context, we define equilibria as temporally steady states of the four state variables N, P, Z and D. They are obtained by setting the left hand side of the related governing ODE system (Eqs. (2) and (3)) to 0. Negative and complex solutions are ignored in our analyzes, because concentrations, as simulated by our models, are naturally positive and real-valued. Moreover, the light limiting term appearing in the ODE systems is not explicitly treated. It represents a constant factor that easily can be added afterwards in the results presented.

The solutions detected are dependent on the parameters in the ODE systems and the initial values y_0. For model LLM, analytic results are obtained, that in particular motivates its separate analysis. The equilibrium solutions presented for models LQM and QQM are in part numerically based.

3.1. Model LLM

For model LLM, there are three real-valued and non-negative solutions analytically identifiable (Eqs. (4)–(6)). Ignoring the quadratic term $\Phi_Z^* \cdot Z^2$, ODE system (2) includes only the nonlinearities caused by the functions J and G and the resulting mathematical problem of four differential equations in four variables is solvable by analytic methods.

The first equilibrium is the solution

$$E^*_{LLM_1} = (N_1^*(S), 0, 0, 0), \tag{4}$$

where N_1^* is a function of the sum of the four initial values $S := \sum y_0$ where y_0 is assumed to be positive. The other states equal 0. Since the ODE system given by Eq. (2) is mass conserving, which means that no external source or sink of nitrogen in any kind exists, N_1^* is simply the accumulated mass of the initial concentrations (see Fig. 2, top). Note, especially, that solution $E^*_{LLM_1}$ is independent of the model parameters.

This solution describes the realistic situation that due to low insolation or due to a low initial nutrient concentration no phytoplankton bloom arises, and consequently neither zooplankton nor detritus reach a significant amount. The lifecycle breaks down

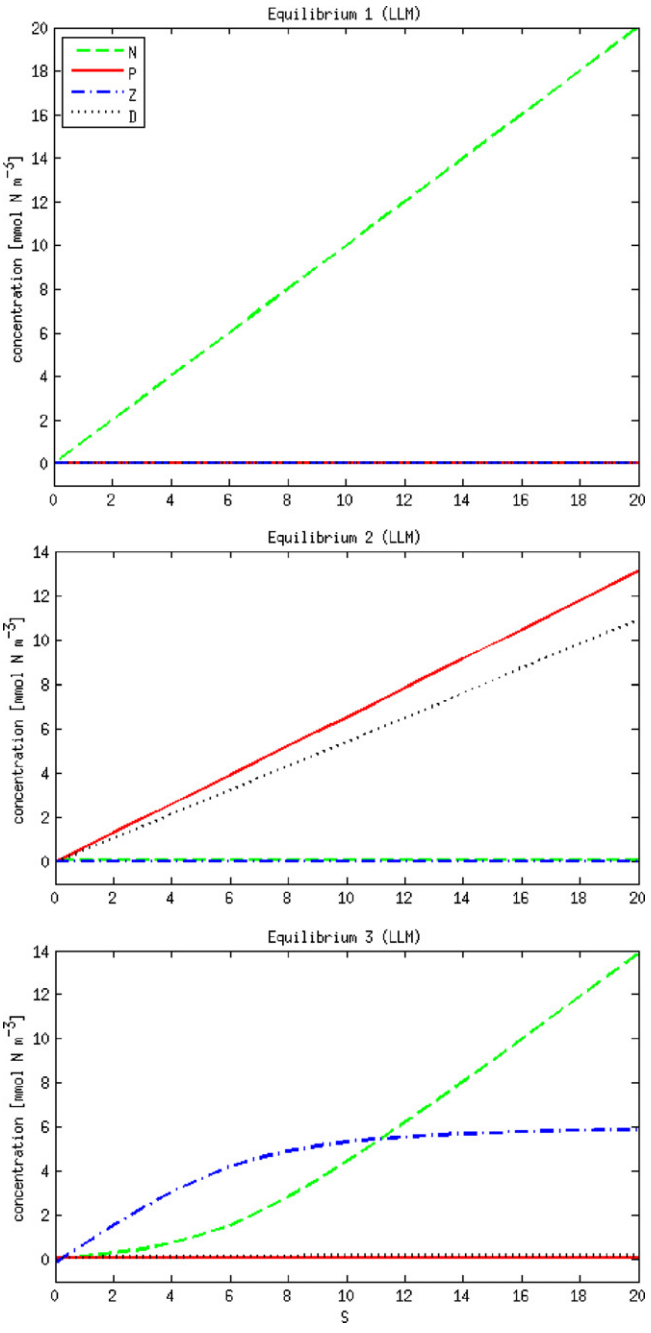

Fig. 2. Equilibrium solutions for model LLM calculated analytically and presented as functions of initial mass S. Parameters are chosen according to Table 1.

resulting in a constant load of free nutrients in the water that is equivalent to the initial mass of the system.

Further reasonable equilibria of system (2) are solutions representing the coexistence of three, or of all four ecosystem components. They are given by

$$E^*_{LLM_2} = \left(\frac{k\Phi_P}{\mu_m - \Phi_P}, P^*_2(S,u), 0, \frac{\Phi_P}{\gamma_m} P^*_2(S,u)\right) \tag{5}$$

and

$$E^*_{LLM_3} = (N^*_3(S,u), P^*_3(u), Z^*_3(S,u), D^*_3(S,u)), \tag{6}$$

where $u \in \mathbb{R}^m$ represents the m parameters included in the model.

$E^*_{LLM_2}$ describes a balanced situation between the three states N, P and D. In this case, D^*_2 is proportional to P^*_2 by a factor Φ_P/γ_m. The state of N^*_2 is no longer dependent on the initial mass, but on the parameter values chosen, in particular on the parameters k, Φ_P and μ_m. Due to the mass conserving property of ODE system (2) mentioned above, the states of phytoplankton and detritus consequently must rely upon the initial mass and an explicit characterization of $P^*_2(S,u)$, due to their relation also of $D^*_2(S,u)$, is obtainable that is given by

$$P^*_2(S,u) = \frac{S - (k\Phi_P/(\mu_m - \Phi_P))}{(\Phi_P/\gamma_m) + 1}. \tag{7}$$

From Eq. (5) the necessary condition $\mu_m > \Phi_P$ is derived to guarantee the non-negativity of solution $E^*_{LLM_2}$. In the opposite situation where the loss of phytoplankton is higher than its growth, phytoplankton would decease in reality and consequently detritus would disappear. This case is already represented by $E^*_{LLM_1}$.

$E^*_{LLM_3}$ describes the situation where all four variables co-exist. All states, except P^*_3, are dependent on the initial mass of nitrogen and on the parameter values chosen. Since the explicit formulations of the three parameter-dependent states are quite long they are given in Appendix A and we restrict our discussion to the state of phytoplankton.

In contrast to the other states, P^*_3 is, similar to N^*_2, only dependent on the parameter values chosen and is defined by

$$P^*_3(u) = \sqrt{\frac{\Phi_Z g}{\epsilon(\beta g - \Phi_Z)}}. \tag{8}$$

Obvious is the fact that due to the positivity of all parameters the condition $\beta g > \Phi_Z$ must be met in order to obtain real values for P^*_3. Further, for the fixed parameters Φ_Z, g, ϵ and β the steady state of P is a constant function in S. Hence, highly variable outcomes of type $E^*_{LLM_3}$ can occur for one initial masses S. Since P^*_3 is fixed by the parameters, there are masses S resulting in solutions in which the compartments of nutrients and detritus dominate, as well as masses that result in solutions where all states range in a similar domain. Even the case that phytoplankton prevails over the other states can be represented by $E^*_{LLM_3}$ for a certain amount of nitrogen S.

Illustrations of equilibria $E^*_{LLM_2}$ and $E^*_{LLM_3}$ are given in the center and on the bottom of Fig. 2, again as functions of initial mass. Here, the equilibrium solutions are computed based on the 'optimal' parameter set found by Schartau and Oschlies (2003) and given in Table 1. The dependencies of the different states among each other are clearly visible. In $E^*_{LLM_2}$, the states of phytoplankton and detritus are dependent on S, increase linearly and are proportional to each other. The states of N and Z are constant with S. In $E^*_{LLM_3}$, P^*_3 is constant while the other three states increase with S. More precisely, zooplankton and detritus converge to a maximum, non-zero value. The compartment of nutrients increases at first exponentially, and for higher values of S almost linearly.

Finally it has to be pointed out that the equilibria presented in this study are all independent on the initial distribution of nitrogen. Dependence on S definitely signifies a sole dependence on the accumulated mass of nitrogen in the system, here represented by the sum S of initial values.

3.2. Model LQM

Due to the quadratic closing term of zooplankton included in model LQM, in contrast to model LLM, for this model analytic solutions of the equilibria are assessable only in part. Assuming $Z^* = 0$, analytic results are still obtained and thus, presented and discussed in the following. The explicit solution of the co-existence equilibrium in which all states are non-zero, however cannot be presented any more. Rational functions of high order, arising as a consequence

of the quadratic loss term added, inhibit explicite calculations of the states. For that reason, the dynamics of this equilibrium solution are analyzed numerically. Individual experiments are performed as well as comparative studies that involve all three models. The latter in particular supports the identification of model characteristics.

As for model LLM, three non-negative and real-valued equilibrium solutions are detected. The first two equilibria of model LQM fully equal the ones of model LLM,

$$E^*_{LQM_1} := E^*_{LLM_1} \quad \text{and} \quad E^*_{LQM_2} := E^*_{LLM_2}, \tag{9}$$

because the models only differ in their formulation of zooplankton loss and in these solutions the state of zooplankton equals 0.

The third equilibrium describes the co-existence of all four marine ecosystem components as it does in model LLM. Caused by the quadratic loss term of zooplankton which is added to this model, explicit expressions of the individual states are not computable any more. More precisely, while in model LLM the state of P^*_3 was independent of S, now all four variables are related to each other which results in mathematically complex terms that only can be treated by introducing further parameters.

A general description of the co-existence solution is given by

$$E^*_{LQM_3} = \left(N^*_3(S,u), P^*_3(S,u), Z^*_3(S,u), D^*_3(S,u)\right). \tag{10}$$

Since explicit expressions of the states cannot be determined, numerical calculations are presented in the following. In particular, results that mirror the effect of initial value variations on the co-existence solution are shown. Comparative experiments of all three models are presented as well to point out individual model characteristics.

Dependent on the initial mass S, the left plot in Fig. 3 depicts numerical calculations of E^*_3 for models LLM and LQM. As before, parameter set u^* given in Table 1 is exemplarily used. Both models show a nearly linear increase in nutrient concentration from a certain concentration on ($S \approx 8\,\mathrm{mmol\,N\,m^{-3}}$ in model LLM and $S \approx 15\,\mathrm{mmol\,N\,m^{-3}}$ in model LQM). Comparing the other states of the two models, however, qualitative differences become obvious. Except N, all states converge asymptotically to a non-zero value with increasing S. But while P^*_3 increases with S in model LQM, it remains constant in model LLM (cp. Section 3.1). Moreover, the states of zooplankton and detritus are almost swapped for this parameter setting for given S. While zooplankton gains significant mass with rising S in model LLM, detritus is the dominant sink of enhanced initial mass in model LQM. Another characteristic of model LQM that arises using parameter set u^* is a rapid change in solution $E^*_{LQM_3}$ at $S' \approx 160\,\mathrm{mmol\,N\,m^{-3}}$ (see Fig. 4). For initial masses $S < S'$, the compartment of N contains most of the mass, for $S > S'$ detritus is the mass domaining compartment. Moreover, with respect to S the slope of P^*_3 increases significantly after this point. For the parameter setup given, this critical point is within a range of nitrogen concentration that is barely interesting for natural applications. By parameter modifications, however, this point may shift towards a realistic range of nitrogen concentrations and hence it may become relevant for model applications.

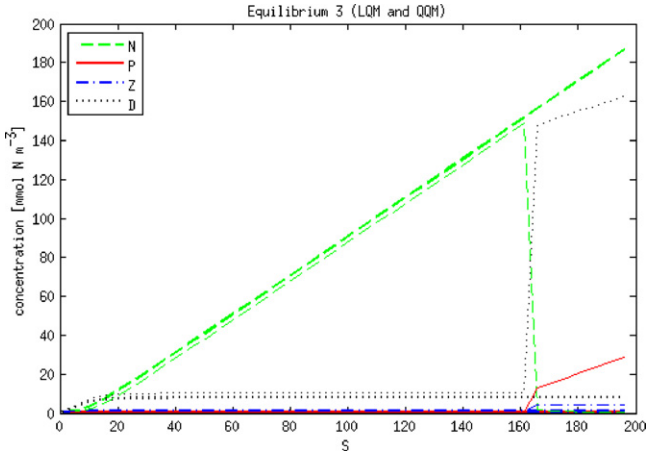

Fig. 4. Numerical calculation of equilibrium E^*_3 for model LQM (thin lines) and model QQM (thick lines). In model LQM a drastic qualitative change occurs at $S \approx 160\,\mathrm{mmol\,N\,m^{-3}}$ in the solution for parametrization u^*.

3.3. Model QQM

Three non-negative and real-valued equilibrium solutions are found for model QQM as well. Since the ODE system given in Eq. (3) is mass conserving just like the system governing the other two models, the first equilibrium of model QQM is equivalent to the first equilibrium of the other models, where N^*_1 is the sum S of the initial masses and $P^*_1 = Z^*_1 = D^*_1 = 0$ (see Eq. (4)). The other two equilibrium solutions differ from the ones presented above. The alteration of the source and sink compartments of phytoplankton and zooplankton entails modified formulations of these solutions. For equilibrium $E^*_{QQM_2}$ parameterized solutions are presented, whereas $E^*_{QQM_3}$ is introduced in a general form.

The second equilibrium of model QQM resembles the one of the other two models. Due to the additional quadratic loss term of

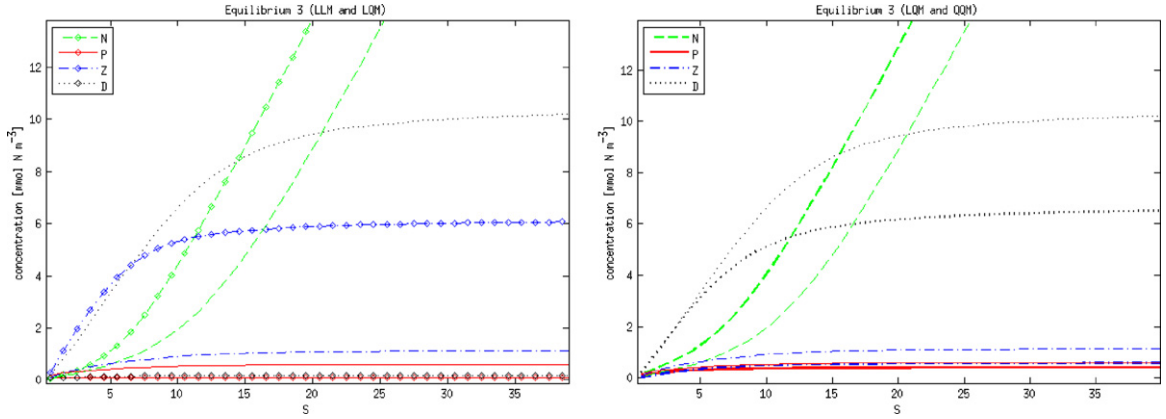

Fig. 3. Numerical calculation of equilibrium E^*_3 given as function of S for model LLM (diamonds) and model LQM (thin lines) on the left, and for models LQM and QQM (thick lines) on the right. Parameter setting as in Fig. 2.

phytoplankton, its formulation however differs and is now given by

$$E^*_{QQM_2} = \left(N^*_2(S,u), P^*_2(S,u), 0, \frac{\Phi^*_P}{\gamma_m} P^*_2(S,u)^2 \right) \tag{11}$$

with

$$N^*_2(S,u) := \frac{k\left(\Phi_P + \Phi^*_P P^*_2(S,u)\right)}{\mu_m - \left(\Phi_P + \Phi^*_P P^*_2(S,u)\right)}.$$

In contrast to the other models, for model QQM N^*_2 is dependent on the parameters u as well as on the initial values S. Furthermore, now D^*_2 is proportional to the square of P^*_2. In model LQM, P^*_2 and D^*_2 are linearly related to each other. These facts cause relations of higher order between the three non-zero states N^*_2, P^*_2 and D^*_2, that inhibit their explicit representation here.

As for model LQM, the third equilibrium, in which all states are nonzero, cannot be determined analytically. It is described by the same general formulation as $E^*_{LQM_3}$ (see Eq. (10)). All equilibrium states vary with both, u and S, and parameter dependent solutions cannot be given any more. Consequently, and similar to model LQM, numerical methods are used to point out characteristics of this solution.

The right plot in Fig. 3 shows numerical solutions of the individual equilibria E^*_3 for models LQM and QQM, again, using parameter set u^*. In contrast to the other two models shown on the left, those two solutions show a qualitatively similar behaviour. Differences are only merely quantitative. For larger initial masses, that are beyond the range shown in Fig. 3, the curves remain close to each other until model LQM shows its change in $E^*_{LQM_3}$. From then on, the solutions differ significantly (see Fig. 4). Particularly, it has to be pointed out that during the experiments described here, neither in the range of S here illustrative presented, nor in any other range, a similar, significant change in solution $E^*_{QQM_3}$ has been detected.

4. Stability of equilibria

The determination of the stability properties of the individual equilibria enables the assessment of model dynamics in dependence of specific parameter settings and initial values. Stability analysis of nonlinear systems is based either on linearizations or on so-called Lyapunov functions. Because in this study the former approach is applied, a brief introduction in the methodology of linearization is given below. For further mathematical details, preconditions required and theorems used, see e.g., Amann (1990). Results with respect to the equilibria presented in the previous section are given subsequently.

Linearization. Given an autonomous, nonlinear IVP (cp. Section 2) with continuously differentiable function $f : \mathbb{R}^n \to \mathbb{R}^n$, its linearization at an equilibrium point y^* is defined by

$$\bar{y}' = J_f(y^*)\bar{y}(t), \tag{12}$$

where $J_f(y^*)$ is the Jacobian of f evaluated at y^*. The resulting linearized system approximates the original, nonlinear system around the equilibrium point. Consequently, statements with respect to the linearization are only locally proven for the original system. From the qualitative theory of linear equations it is known that the dynamics of the system described by Eq. (12) are related to the eigenvalues $\lambda = \alpha + i\beta$ of $J_f(y^*)$. For linear systems, two main qualitative distinctions can be made based on the eigenvalues' real parts α (see below).

- In case $\alpha \leq 0$ for all λ, the linear system tends towards the equilibrium solution y^* and y^* is termed stable.[1]
- In case $\alpha > 0$ for at least one λ, the linear system drifts away from the equilibrium solution y^* and y^* is termed unstable.

This criterion is denoted by (*C*) in the following. Provided that the eigenvalues of $J_f(y^*)$ meet either the first case and in particular $\alpha < 0$ holds, or the second case, the corresponding stability statement can be directly transferred from the linearization to the original, nonlinear model (cp. Amann, 1990). However, in case $\alpha \leq 0$ for all λ and $\alpha = 0$ for at least one λ, further analyses are necessary to evaluate the quality of y^* in the original system.

In the following, we refer to the linearizations of the ODE systems presented in Section 2 at an equilibrium solution y^* as $J_L(y^*)$ for models LLM and LQM and $J_Q(y^*)$ for model QQM. The existence of these linearizations is ensured through the continuous differentiability of both ODE systems. For $i = 1, 2, 3$, the eigenvalues of the respective linearization are summarized in the vector $\lambda_{<model>_i} := (\lambda_1, \lambda_2, \lambda_3, \lambda_4)$.

4.1. Model LLM

The Jacobian of system (2), J_L, is evaluated at the three equilibrium solutions $E^*_{LLM_i}$, $i = 1, 2, 3$ presented in the previous section. The eigenvalues of $J_L(E^*_{LLM_1})$ and $J_L(E^*_{LLM_2})$ are calculated analytically, whereas the eigenvalues λ_{LLM_3} are computed numerically.

For $J_L(E^*_{LLM_1})$, the eigenvalues are given by

$$\lambda_{LLM_1} = \left(0, -\Phi_Z, -\gamma_m, -\frac{k\Phi_P - \mu_m S + \Phi_P S}{k+S}\right). \tag{13}$$

It becomes obvious that λ_1 is zero and λ_2 and λ_3 are negative for every parameter setting and all initial values. Only λ_4 can be either negative or positive, dependent on the amount of nitrogen in the system and the parameters chosen. Looking at Eq. (13), it can be seen that in particular only parameters that are related to phytoplankton growth, namely k, Φ_P and μ_m, affect the quality of solution $E^*_{LLM_1}$. Further, explicit parameter conditions can be derived from Eq. (13) that specify the quality of $E^*_{LLM_1}$.

The eigenvalues belonging to the solutions $E^*_{LLM_2}$ and $E^*_{LLM_3}$ are presented in a more general way. For λ_{LLM_2} explicit results are obtained, but they are lengthy and not instructive any more (see Appendix A). The eigenvalues λ_{LLM_3} are not analytically calculable any more. To identify nonetheless initial value and parameter conditions that predetermine the quality of the two latter equilibria, numerical experiments were conducted for different parameter settings u. First of all, it has to be remarked that in both, λ_{LLM_2} and λ_{LLM_3} one eigenvalue generally equals 0, just as in λ_{LLM_1}. Thus, the eigenvalue sets λ_{LLM_2} and λ_{LLM_3} are represented by

$$\lambda_{LLM_i} = (0, \lambda_2(S,u), \lambda_3(S,u), \lambda_4(S,u)) \tag{14}$$

for $i = 2, 3$. To determine the domains in which the equilibria are stable or unstable, numerical calculations of the eigenvalues of the linearizations are compared for various initial masses S. Table 2 shows the eigenvalues' real parts for linearization $J_L(E^*_{LLM_1})$, $J_L(E^*_{LLM_2})$ and $J_L(E^*_{LLM_3})$. Parameters are chosen according to Table 1. Following criterion (*C*), equilibrium $E^*_{LLM_1}$ is unstable for all initial masses except $S = 0$. The model does not simulate the sole existence of free nitrogen. For $E^*_{LLM_2}$ and $E^*_{LLM_3}$, there are initial masses resulting in the negativity of all eigenvalues except λ_1, but also initial masses ensuring the instability of the respective solution.

[1] Note, that there is a mathematical distinction between stability and asymptotical stability. Here, we claim only the former.

Table 2
Real parts of the eigenvalues for model LLM calculated analytically (λ_{LLM_1} and λ_{LLM_2}) and numerically (λ_{LLM_3}) for varied initial masses S and fixed parameters according to Table 1.

S	λ_{LLM_1}				λ_{LLM_2}				λ_{LLM_3}			
0	0	−0.0100	−0.0480	−0.0400	0	−0.0095	−0.0585	0.0313	0	−0.0757	−0.0757	0.0285
0.1	0	−0.0100	−0.0480	0.0666	0	−0.0081	−0.0438	−0.0438	0	−0.0721	−0.0721	0.0123
0.2	0	−0.0100	−0.0480	0.1496	0	0.0020	−0.0740	−0.0740	0	−0.0694	−0.0694	−0.0018
0.3	0	−0.0100	−0.0480	0.2159	0	0.0204	−0.1042	−0.1042	0	−0.0684	−0.0684	−0.0127
1	0	−0.0100	−0.0480	0.4618	0	0.3103	−0.5352	−0.0959	0	−0.0881	−0.0881	−0.0350
5	0	−0.0100	−0.0480	0.7083	0	1.2745	−2.9573	−0.0892	0	−0.4336	−0.0669	−0.0384
10	0	−0.0100	−0.0480	0.7573	0	1.3999	−5.9773	−0.0886	0	−0.6644	−0.0241	−0.0487
20	0	−0.0100	−0.0480	0.7842	0	1.4349	−12.0163	−0.0883	0	−0.7405	−0.0211	−0.0481
40	0	−0.0100	−0.0480	0.7984	0	1.4439	−24.0937	−0.0881	0	−0.7641	−0.0208	−0.0480

Using parameter set u^* for example, $E^*_{LLM_3}$ is unstable for small initial masses, while $E^*_{LLM_2}$ is unstable for larger masses of nitrogen S.

Looking at the eigenvalues of all three linearizations, it is conspicuous that for given S two linearizations have a positive eigenvalue. Thus, following criterion (C), two of the three equilibria considered are unstable relating to their linearization as well as relating to the original, nonlinear system. The largest eigenvalue of the remaining linearization equals 0. In this case, criterion (C) only makes a statement reffering to the linearization, but not referring to the original, nonlinear system. The quality of the solution in the latter case is thus further analyzed numerically.

Fig. 5 shows the output of two simulation runs of model LLM for initial mass $S_1 = 0.1\,\mathrm{mmol\,N\,m^{-3}}$ (top) and for initial mass $S_2 = 2.0\,\mathrm{mmol\,N\,m^{-3}}$ (center). S_1 represents the stable domain of $E^*_{LLM_2}$ in the linearized system, S_2 is representative for the stable range of $E^*_{LLM_3}$. On the left, the simulation is shown over time, and phase curves N vs. P and Z vs. D are given on the right. For S_1 the model asymptotically tends towards $E^*_{LLM_2}$. It is well recognizable that the state of zooplankton converges to zero whereas the other states converge to a non-zero value. Equally to its behaviour in the linearized system, solution $E^*_{LLM_2}$ shows stable behaviour in the original system for small initial masses. Initializing the model with a higher mass of nitrogen (S_2), all variables converge to non-zero values. Thus, a similar situation appears as before, but with respect to $E^*_{LLM_3}$.

Other numerical experiments performed (not shown here) indicate a smooth transition from one to another equilibrium with increasing S, which is investigated for the linearized system as well as for the original, nonlinear system. Moreover, it seems likely that from a certain threshold S_T on, for all $S \geq S_T$ the model dynamics are determined by the co-existence equilibrium $E^*_{LLM_3}$.

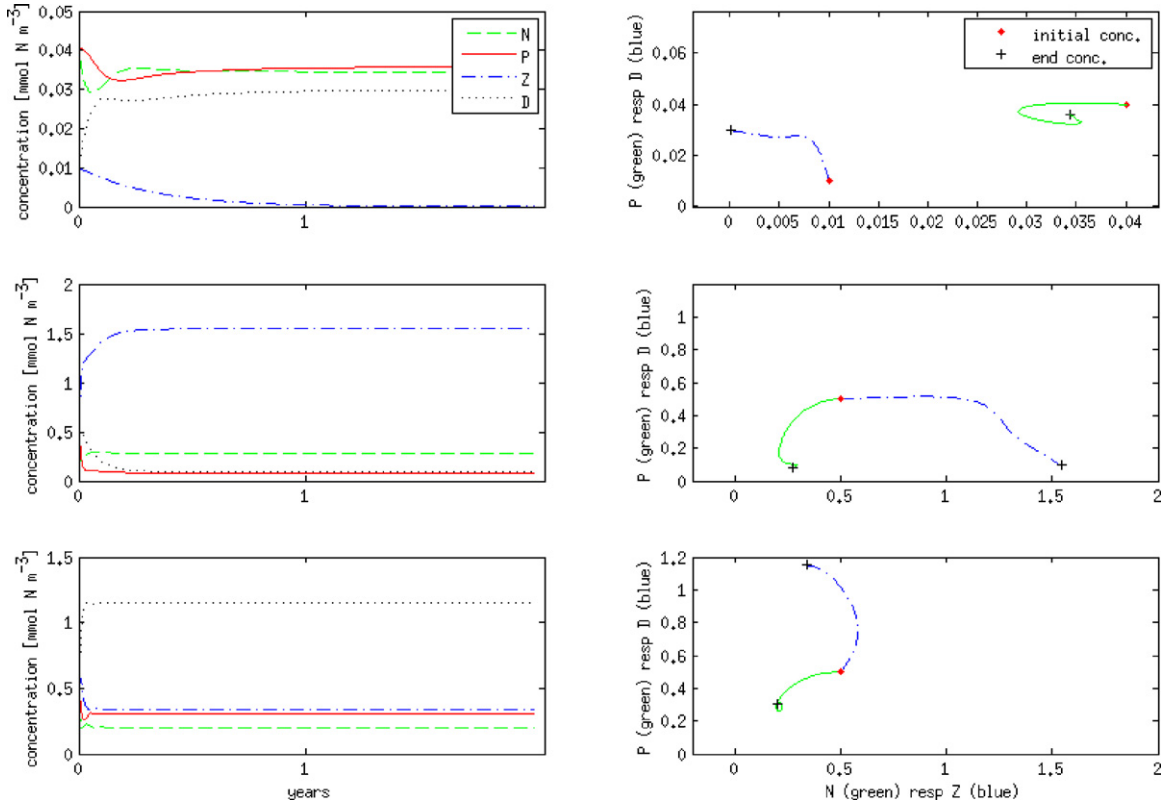

Fig. 5. Simulation of model LLM (top, middle) and LQM (bottom) for initial mass $S_1 = 0.1\,\mathrm{mmol\,N\,m^{-3}}$ (top) and initial mass $S_2 = 2.0\,\mathrm{mmol\,N\,m^{-3}}$ (middle, bottom). On the left, the simulations over time, on the right, phase portraits of N vs. P (green, solid line) and Z vs. D (blue, dash-dotted line). Initial concentrations are marked by a red dot, end concentrations are marked by a black cross. (For interpretation of colour in the artwork, the reader is referred to the web version of the article.)

4.2. Model LQM

For model LQM we gained results similar to the results for model LLM. Since $E^*_{LLM_i} = E^*_{LQM_i}$ for $i = 1, 2$ and both solutions imply $Z = 0$, the respective eigenvalues agree. The eigenvalues of $E^*_{LQM_3}$ differ from the ones associated to model LLM and have to be calculated numerically.

$$\lambda_{LQM_1} = \lambda_{LLM_1} \quad \text{and} \quad \lambda_{LQM_2} = \lambda_{LLM_2}. \tag{15}$$

The eigenvalues of $E^*_{LQM_3}$ can only be calculated numerically.

For parameter set u^*, results are exemplary given in Fig. 5 Consistent to our analytic results, model LQM returns the same outcome as model LLM when initialized with mass S_1. Thus, its graph coincides with the graph shown at the top left of Fig. 5. The initialization with S_2 results in an outcome distinct to the outcome presented for model LLM. But as for model LLM, this initialization clearly engenders a convergence towards the co-existence solution E^*_3 (see Fig. 5, bottom).

4.3. Model QQM

Equilibrium $E^*_{QQM_1}$ equals the first equilibrium of the other two models and the respective linearizations agree as well. Consequently, the corresponding eigenvalues are the same.

The other equilibria detected for model QQM, however, differ from the ones discussed above. In contrast to the second equilibrium of the first models, all states of $E^*_{QQM_2}$ already depend on both, the parameters u and initial mass S. For models LLM and LQM this is true only for the co-existence solution. Furthermore, in $E^*_{QQM_2}$ an internal, quadratic dependence of the states appears. Both facts together lead to a complicated explicit formulation of the states in $E^*_{QQM_2}$ making an analytic calculation of the respective eigenvalues for the second equilibrium unfeasible.

Thus, to assess the stability domains of the equilibrium solutions $E^*_{QQM_i}$, $i = 2, 3$ without any knowledge of the analytic formulation of the eigenvalues, numerical experiments with respect to variations in S are performed. Comparative experiments with model LLM and model LQM are conducted as well to check the models on dynamic similarities. Subject to initial mass S, Fig. 6 illustrates the transition from one equilibrium to another, on the left shown for models LLM and LQM, on the right for model QQM. Vertical lines constitute critical values S^* where the quality of an equilibrium changes. The smooth transition between the stable states pictured is attributed to numerics.

For models LLM and LQM the critical values could be identified analytically by calculating the zeros of the explicit expressions of λ_{LLM_i}, $i = 1, 2$. Using parameter set u^* the stability of E^*_1 and E^*_2 changes at $S^*_1 = 0.0344\,\mathrm{mmol\,N\,m^{-3}}$. For $S < S^*_1$ the former is stable while for larger S, E^*_2 is stable. A second critical value that is related to a stability transition from E^*_2 to E^*_3 appears at $S^*_2 = 0.1857\,\mathrm{mmol\,N\,m^{-3}}$. Further stability changes are not detected for this parameter setting, thus E^*_3 is stable for all $S > S_2$. However, other parameter combinations (not explicitly presented here) show a further quality change in E^*_3. A third critical value S^*_3 is found where the quality of E^*_3 turns back from stable to unstable. This event however does not result in the stability of another equilibrium, as it does at the critical values previously described, but to oscillations around E^*_3 that are stable. For details on this phenomenon, called limit sets, see e.g., Amann (1990).

The eigenvalues λ_{QQM_1} coincide with the eigenvalues of J_L evaluated at the first equilibrium of the other two models. Thus, for model QQM the first transition occurs at $S^*_1 = 0.0344\,\mathrm{mmol\,N\,m^{-3}}$ as well. The second critical value could not be detected precisely for model QQM since neither λ_{QQM_2} nor λ_{QQM_3} could be calculated analytically. Numerical experiments indicate a transition from the second to the third equilibrium at $S \in [0.25, 0.3]\,\mathrm{mmol\,N\,m^{-3}}$, in Fig. 6 marked by a dashed, vertical line.

5. Discussion

The basic dynamics of three models of the marine ecosystem are analyzed mathematically using the qualitative theory of dynamical systems. Equilibria and their stability dependent on initial values and parameters are determined. From this, parameter conditions as well as ranges of initial values are identified that lead to a specific quality of the model output. In addition, comparative studies are conducted that support the identification of model characteristics caused by their distinct formulations of phytoplankton loss and zooplankton loss.

For each model, three non-negative and real equilibrium solutions are determined. The first equilibrium solution, E^*_1, is the same for all three models. It represents a situation where nutrients are available in the system, but there is no organism using them. Its range of stability depends on the initial mass S as well as on the parameters k, Φ_P and μ_m. In case the mortality rate of phytoplankton is larger than its growth rate, $\Phi_P > \mu_m$, this state is stable for all masses of nitrogen S. In case $\Phi_P < \mu_m$ a critical value S^* exists, that for all initial masses $S > S^T$ this solution is unstable and another equilibrium solution of the respective model is targeted. For the parameter set exemplarily used in this study, solution E^*_2 of the models become stable from this point. It has to be remarked, however, that for other parameter setups, e.g., in case equilibrium E^*_2 does not have a positive and real-valued solution due to parameter relations (compare Section 3), the models show a different behaviour.

Equilibrium E^*_2 depicts a balanced situation between nutrients, phytoplankton and detritus for all three models. Zooplankton does not survive in this solution. The explicit expression of E^*_2 depends on the underlying ODE system. For models LLM and LQM the expressions equal since they are based on the same ODE system and $Z = 0$ holds in this equilibrium. In this equilibrium, the states of P^*_2 and D^*_2 are functions of initial mass S and of the parameters

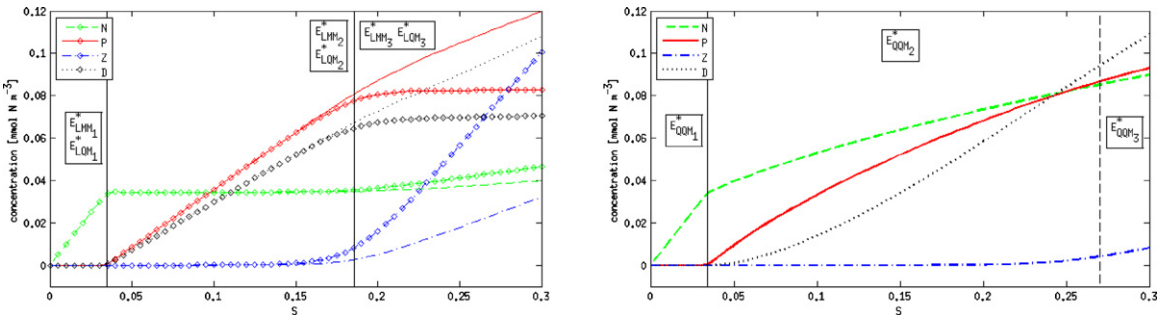

Fig. 6. Numerically computed, stable equilibria E^*_{LLM} and E^*_{LQM} on the left, and E^*_{QQM} on the right, as functions of initial mass S. Critical values S^* are marked by vertical lines (solid = analytically calculated, dashed = numerically estimated).

k, Φ_P, μ_m and γ_m. Both states increase linearly with N and thus, with S. For model QQM, the states P_2^* and D_2^* are dependent on the variables mentioned as well, but are additionally dependent on the quadratic mortality parameter Φ_P^*. Furthermore, in contrast to models LLM and LQM, there are quadratic interrelations between the single states that result in elusive state expressions and pointing out definite parameter relations is not practical anymore.

For models LLM and LQM the stable domains of the second equilibria can be computed analytically. Explicit parameter and initial value dependencies however are not presented since the internal coherencies are too complex to allow instructive statements. Instead, numerical experiments are conducted and exemplary results for parameter set u^* are presented. As mentioned above, the results show that E_2^* becomes stable the moment E_1^* becomes unstable. For model QQM the same behaviour is found. For very small values of S, $E_{QQM_2}^*$ is unstable and $E_{QQM_1}^*$ is stable. At a critical mass of nitrogen S_1^* specified by the parameters k, Φ_P and μ_m, the quality of $E_{QQM_2}^*$ changes and the solution becomes stable. At a point S_2^* the solution becomes unstable again and from here, the third equilibrium determines the model outcome.

The expression of the third equilibrium is specific for each model. Analytic solutions are obtained only for model LLM, the other co-existence equilibria are investigated numerically. Most conspicuous is the fact that for model LLM the state P^* is constant with varying initial masses S in E_3^*. This is in contrast to the more complex models, models LQM and QQM, wherein all states, in particular P^*, are related to S. Furthermore, for model LLM the condition $\beta g > \Phi_Z$ is revealed that is required to obtain real-valued solutions of type E_3^*.

Due to the constant state P^* for various S in model LLM the outcome differs significantly from the outcome of the models LQM and QQM in case the co-existence of all four variables is simulated. All three models show a nearly linear increase of nutrients and an asymptotical increase of the states Z and D as soon as solution E_3^* is responsible for the model outcome. Simultaneously however, P is constant in model LLM, while it increases asymptotically with increasing mass in models LQM and QQM. Moreover, in model LLM the compartment of zooplankton dominates over the states of phytoplankton and detritus. In the other two models, models LQM and QQM, detritus prevails.

The range of stability of solution E_3^*, related to initial mass S, is similar for all models. While the solution is unstable for small values of S and instead E_1^* or E_2^* are stable, at a certain value S^* its quality changes from unstable to stable. From this point, solution E_3^* either keeps stable or it becomes the center of a stable limit set, dependent on the parameter set chosen. For the exemplary parameter set u^* the former case occurs. One restriction has to be pointed out regarding model LLM. As mentioned above, the condition $\beta g > \Phi_Z$ must be met to ensure the reasonability of solution $E_{LLM_3}^*$. Appropriately, the stability of $E_{LLM_3}^*$ is related to this inequality as well. Once the condition is satisfied, the quality of $E_{LLM_3}^*$ is as described above. Otherwise, $E_{LLM_3}^*$ is unstable for all S and instead, $E_{LLM_2}^*$ keeps stable also for higher values of S. For the other two models we did not find a similar feature.

6. Conclusions

Knowing the basic dynamics of a model, depicted by its equilibrium solutions, it is possible to determine the model's behaviour under specific conditions. According to the results presented here, qualitatively high differences in the equilibrium solutions can occur due to simple modifications of the governing equations (cp. model LLM and model LQM). However, it is also possible that this kind of modifications do not affect the quality of the solutions significantly (cp. models LQM and QQM). We thus conclude that a general transfer of results regarding the model behaviour from one model formulation to another is not possible. The analysis of a model's framework, however, helps to understand the potential differences of the model results and enables the deduction of specific model characteristics. In particular, our findings help to restrict the parameter space in the course of data assimilation and to reveal limits of the model to reproduce certain data sets. Moreover, conclusions on the impact of external forcings, such as nutrient supply due to the modelling of a seasonal varying mixed layer depth, are enabled.

Appendix A.

A1. The equilibrium states of nutrients, zooplankton and detritus in solution $E_{LLM_3}^*$ are explicitly given by

$$\begin{aligned}
N_3^*(S,u) &= -[\theta_1 - ((\theta_1 + \gamma_m k\Phi_Z - \gamma_m\Phi_Z S)^2 \\
&\quad + 4\gamma_m k\Phi_Z(\gamma_m\Phi_Z S - \gamma_m\Phi_Z\theta_2 + \beta\gamma_m\Phi_P\theta_2 - \beta\Phi_P\Phi_Z P_3^*))^{1/2} \\
&\quad + \gamma_m k\Phi_Z - \gamma_m\Phi_Z S]\cdot[2\gamma_m\Phi_Z]^{-1}, \\
Z_3^*(S,u) &= \frac{\beta(\Phi_P + [\mu_m\theta_2]\cdot[2\gamma_m\Phi_Z(k - (\theta_2/2\gamma_m\Phi_Z))]^{-1})P_3^*}{\Phi_Z}, \\
D_3^*(S,u) &= \frac{(\beta\Phi_P + [\mu_m(\beta-1)\theta_2]\cdot[2\gamma_m\Phi_Z(k - (\theta_2/2\gamma_m\Phi_Z))]^{-1})P_3^*}{\gamma_m},
\end{aligned}$$

where

$$\begin{aligned}
\theta_1 &= P_3^*(\gamma_m\Phi_Z + \Phi_Z\mu_m - \beta\gamma_m\Phi_P + \beta\gamma_m\mu_m + \beta\Phi_P\Phi_Z - \beta\Phi_Z\mu_m), \\
\theta_2 &= \theta_3 + \gamma_m\Phi_Z(k - y_0) - ((\theta_3 + \gamma_m k\Phi_Z - \gamma_m\Phi_Z S)^2 \\
&\quad + 4\gamma_m k\Phi_Z(\gamma_m\Phi_Z S - \gamma_m\Phi_Z P_3^* + \beta\gamma_m\Phi_P P_3^* - \beta\Phi_P\Phi_Z P_3^*))^{1/2}, \\
\theta_3 &= P_3^*\cdot(\gamma_m\Phi_Z + \Phi_Z\mu_m - \beta\gamma_m\Phi_P + \beta\gamma_m\mu_m + \beta\Phi_P\Phi_Z - \beta\Phi_Z\mu_m),
\end{aligned}$$

and P_3^* as presented in Section 3.1.

A2. The non-zero eigenvalues of λ_{LLM_2} are quite elusive and we only write down the simplest one, λ_2, in detail. The explicit depiction of the other two eigenvalues is not reasonable.

$$\begin{aligned}
\lambda_2 = &-[g\Phi_P^4\Phi_Z + 2g\gamma_m\Phi_P^3\Phi_Z - 2g\Phi_P^3\Phi_Z\mu_m \\
&+ g\gamma_m^2\Phi_P^2\Phi_Z + g\gamma_m^2\Phi_Z\mu_m^2 + g\Phi_P^2\Phi_Z\mu_m^2 \\
&+ \epsilon\gamma_m^2k^2\Phi_P^2\Phi_Z + \epsilon\gamma_m^2\Phi_P^2\Phi_Z S^2 + \epsilon\gamma_m^2\Phi_Z\mu_m^2S^2 \\
&+ 2g\gamma_m\Phi_P\Phi_Z\mu_m^2 - 4g\gamma_m\Phi_P^2\Phi_Z\mu_m - 2g\gamma_m^2\Phi_P\Phi_Z\mu_m \\
&- \beta\epsilon g\gamma_m^2\mu_m^2S^2 + 2\epsilon\gamma_m^2k\Phi_P^2\Phi_Z S - 2\epsilon\gamma_m^2\Phi_P\Phi_Z\mu_m S^2 \\
&- \beta\epsilon g\gamma_m^2k^2\Phi_P^2 - \beta\epsilon g\gamma_m^2\Phi_P^2S^2 - 2\beta\epsilon g\gamma_m^2k\Phi_P^2S \\
&+ 2\beta\epsilon g\gamma_m^2\Phi_P\mu_m S^2 - 2\epsilon\gamma_m^2k\Phi_P\Phi_Z\mu_m S \\
&+ 2\beta\epsilon g\gamma_m^2k\Phi_P\mu_m S]/[\epsilon\gamma_m^2k^2\Phi_P^2 \\
&+ 2\epsilon\gamma_m^2k\Phi_P^2S - 2\epsilon\gamma_m^2k\Phi_P\mu_m S + \epsilon\gamma_m^2\Phi_P^2S^2 + g\gamma_m^2\Phi_P^2 \\
&- 2\epsilon\gamma_m^2\Phi_P\mu_m S^2 - 2g\gamma_m^2\Phi_P\mu_m + \epsilon\gamma_m^2\mu_m^2S^2 + g\gamma_m^2\mu_m^2 \\
&+ 2g\gamma_m\Phi_P^3 - 4g\gamma_m\Phi_P^2\mu_m + 2g\gamma_m\Phi_P\mu_m^2 + g\Phi_P^4 \\
&- 2g\Phi_P^3\mu_m + g\Phi_P^2\mu_m^2].
\end{aligned}$$

References

Amann, H., 1990]. Ordinary Differential Equations: An Introduction to Nonlinear Analysis. Walter de Gruyter.

Denman, K.L., Peña, M.A., 1999]. A coupled 1-D biological/physical model of the northeast subarctic Pacific Ocean with iron limitation. In: Deep Sea Research II, vol. 46, pp. 2877–2908.

Edwards, A.M., 2001]. Adding detritus to a nutrient–phytoplankton–zooplankton model: a dynamical approach. Journal of Plankton Research 23, 389–413.
Fan, W., Lvasham, X., 2009]. Data assimilation in a simple marine ecosystem model based on spatial biological parameterizations. Ecological Modelling 220, 1997–2008.
Fasham, M.J.R., 1995]. Variations in the seasonal cycle of biological production in subarctic oceans: a model sensitivity analysis. In: Deep Sea Research I, vol. 42, pp. 1111–1149.
Fasham, M.J.R., Flynn, K.J., Pondaven, P., Anderson, T.R., Boyd, P.W., 2006]. Development of a robust marine ecosystem model to predict the role of iron in biogeochemical cycles: a comparison of results for iron-replete and iron-limited areas, and the SOIREE iron-enrichment experiment. In: Deep Sea Research I, vol. 53, pp. 333–366.
Fennel, K., Losch, M., Schröter, J., Wenzel, M., 2001]. Testing a marine ecosystem model: sensitivity analysis and parameter optimization. Journal of Marine Research 28, 45–63.
Gibson, G.A., Musgrave, D.L., Hinckley, S., 2005]. Non-linear dynamics of a pelagic ecosystem model with multiple predator and prey types. Journal of Plankton Research 27, 427–447.
Gregg, W.W., Ginoux, P., Schopf, P.S., Casey, N.W., 2003]. Phytoplankton and iron: validation of a global three-dimensional ocean biogeochemical model. In: Deep Sea Research II, vol. 50, pp. 3143–3169.
Hinckley, S., Coyle, K.O., Gibson, G., Hermann, A.J., Dobbins, E.L., 2009]. A biophysical NPZ model with iron for the Gulf of Alaska: reproducing the differences between an oceanic HNLC ecosystem and a classical northern temperate shelf ecosystem. In: Deep Sea Research II, vol. 56, pp. 2520–2536.
Kawamyko, M., 2002]. Numerical model approaches to address recent problems on pelagic ecosystems. Journal of Oceanography 58, 365–378.
Kriest, I., Khatiwala, S., Oschlies, A., 2010]. Towards an assessment of simple global marine biogeochemical models of different complexity. Progress in Oceanography 86, 337–360.
López-Fidalgo, J., Wong, W.K., 2002]. Design issues for the Michaelis–Menten model. Journal of Theoretical Biology 215, 1–11.
Losa, S.N., Vézina, A., Wright, D., Lu, Y., Thompson, K., Dowd, M., 2006]. 3D ecosystem modelling in the North Atlantic: relative impacts of physical and biological parametrizations. Journal of Marine System 61, 230–245.
McCreary, J.P., Kohler, K.E., Hood, R.R., Smith, S., Kindle, J., Fischer, A.S., Weller, R.A., 2001]. Influences of diurnal and intraseasonal forcing on mixed-layer and biological variability in the central Arabian Sea. Journal of Geophysical Research 106, 7139–7155.
Moore, J.K., Doney, S.C., Glover, D.M., Fung, I.Y., 2002]. Iron cycling and nutrient-limitation patterns in surface waters of the World Ocean. In: Deep Sea Research II, vol. 49, pp. 463–507.
Murray, A.G., Parslow, J.S., 1999]. The analysis of alternative formulations in a simple model of a coastal ecosystem. Ecological Modelling 119, 149–166.
Oschlies, A., Garçon, V., 1999]. An eddy-permitting coupled physical–biological model of the North Atlantic. 1. Sensitivity to advection numerics and mixed layer physics. Global Biogeochemical Cycles 13, 135–160.
Pahlow, M., Vežina, A.F., Casaul, B., Maass, H., Malloch, L., Wright, D., Lu, Y., 2008]. Adaptive model of plankton dynamics for the North Atlantic. Progress in Oceanography 76, 151–191.
Rückelt, J., Sauerland, V., Slawig, T., Srivastav, A., Ward, B., Patvardhan, C., 2010]. Parameter optimization and uncertainty analysis in a model of oceanic CO_2 uptake using a hybrid algorithm and algorithmic differentiation. Nonlinear Analysis: Real World Applications 11, 3993–4009.
Schartau, M., Oschlies, A., 2003]. Simultaneous data-based optimization of a 1D-ecosystem model at three locations in the North Atlantic: Part I. Method and parameter estimates. Journal of Marine Research 61, 765–793.
Spitz, Y.H., Newberger, P.A., Allen, J.S., 2003]. Ecosystem response to upwelling off the Oregon coast: behavior of three nitrogen-based models. Journal of Geophysical Research 108, 3062.